Turbulent Drag Reduction of Polymeric Solutions

E. R. VAN DRIEST*
North American Rockwell Corporation, Downey, Calif.

The paper presents the results of a comprehensive analytical and experimental program on the effect of additives, mainly long-chain molecules, on drag reduction in turbulent flow of aqueous polymeric solutions. The intent of the study was to develop a basic understanding, deduced from the experimental observations, of the underlying physical mechanism responsible for the phenomenon. The paper assumes that the turbulent drag reduction of solutions of high polymers is because of the damping of turbulent fluctuations by the interspersed polymers, thereby suppressing the generation of turbulence in the viscous sublayer of the flow. Transition itself would also be restrained at sufficiently great polymer concentrations. The basic experiment is the measurement of the friction factor vs Reynolds number for flow in a pipe for various concentrations of a given polymer dissolved in water. The experimental data on drag reduction are interpreted in terms of additive concentration, pipe diameter, and a hydraulic damping thickness analogous to the hydraulic roughness of rough surfaces. Formulas are accordingly derived for velocity profile and friction factor.

Nomenclature

μ = viscosity
μ_0 = viscosity at zero concentration
p = concentration, ppm by weight
c = concentration, g/cm^3
N_0 = Avogadro's number
M = molecular weight
$\tilde{l}$ = length of polymer molecule
d = diameter of polymer molecule
d_s = diameter of sphere
v = volume
ρ = density
τ_w = shear stress at wall
D = diameter of pipe
L = thickness of damping layer
δ = thickness of viscous sublayer
f = friction factor, $8\ \tau_w/\rho V^2$
V = average velocity
Re_D = $\rho VD/\mu$
A = const
B = const
l = mixing length
k = Kàrmàn constant in $l = ky$
k' = modified Kàrmàn constant in $l = k'y$
y = distance from wall
u = local velocity
u_m = maximum velocity in pipe
u^* = $u/(\tau_w/\rho)^{1/2}$
y^* = $\rho(\tau_w/\rho)^{1/2}y/\mu$
L^* = $\rho(\tau_w/\rho)^{1/2}L/\mu$

Introduction

THE reduction in drag of turbulent flow by introduction of foreign matter into the fluid is a relatively recent phenomenon particularly attractive to engineers involved with drag of fluids in and around bodies, as well as to students of turbulent flow itself. This "Toms" effect is strikingly demonstrated when small amounts of certain long-chain molecules (polymers) are dissolved in water. While much is currently being written on the subject, the report by Hoyt and Fabula[1] presents a clear description of the friction reducing phenomenon and gives a brief review of the literature to that time. More recently, a symposium organized by Wells[2] further consolidated the state of knowledge on viscous drag reduction.

The present paper reports results of experiments with a number of high-molecular-weight polymers, namely, Guar Gum, Poly(ethylene oxide) (Polyox) WSR N-750, WSR-205, and WSR-301. Aqueous solutions of these polymers were tested in a number of pipe sizes, $\frac{1}{4}$-, $\frac{1}{2}$-, and 1-in. diam. In an important part of the program, the temperature was also varied so that tests were conducted on some of the polymers with cold, warm, and hot water in the $\frac{1}{2}$-in. tube.

Fundamentally, the purpose of the program described in this report was to throw light on the mechanism by which the additives in the form of long-chain molecules restrain the turbulent motion, thereby reducing drag at high Reynolds numbers. Such knowledge and ideas could presumably be extended to turbulent drag reduction in other fluid media.

Experiment and Analysis

Experiments were conducted mainly on flow in glass tubes to determine the friction factor as a function of Reynolds number as well as polymer concentration. Figure 1 shows

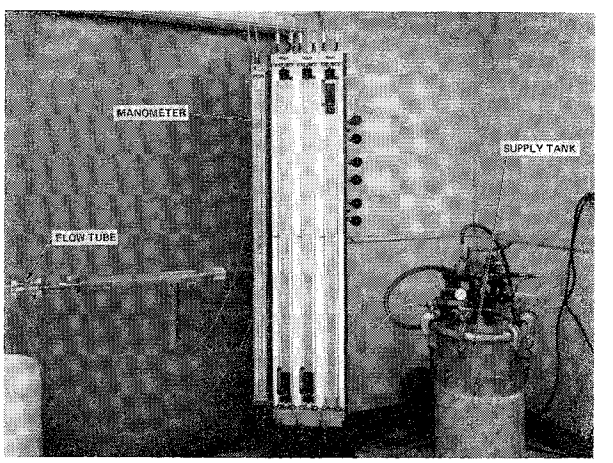

Fig. 1 View of experimental apparatus.

Presented as Paper 70-56 at the AIAA 8th Aerospace Sciences Meeting, New York, January 19–21, 1970; submitted March 2, 1970; revision received May 11, 1970. This research was supported by the U.S. Air Force through the Air Force Office of Scientific Research of the Office of Aerospace Research under Contract AF 49(638)-1442. The author gratefully acknowledges the assistance of D. A. Jones and W. Lubahn in carrying out the laboratory experiments.

* Scientific Advisor, Flight Technology. Member AIAA.

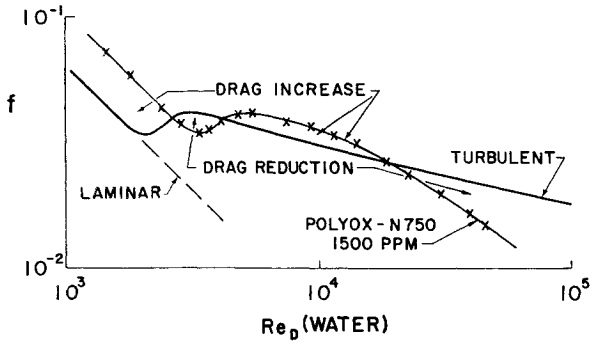

Fig. 2 Friction factor for 1500-ppm aqueous solution of polyox-N750 in ½-in. pipe; Reynolds number based on water viscosity; temperature 70°F.

the simple system, including pressurized supply tank, manometer board, flow tube, and catch basin. The system was open so that the polymer solution was forced through the pipe under pressure atop the solution in the supply tank. This way, there was minimum danger of damage to the macromolecules flowing through the tube. The flow velocity was obtained by weighing the exiting flow with a stopwatch.

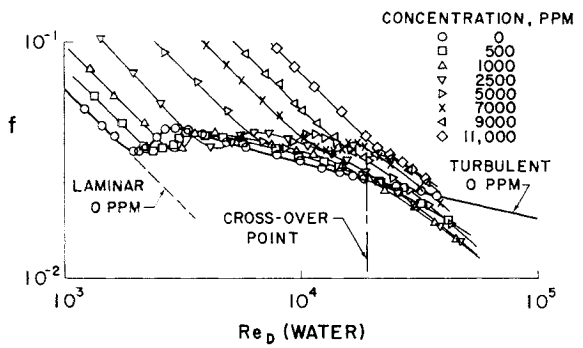

Fig. 3 Friction factor for aqueous solutions of Polyox-N750 in ½-in. pipe; Reynolds number based on water viscosity; temperature 71°F.

Typical are the data shown in Fig. 2 for 1500 ppm Polyox N-750 of molecular weight 300,000. The heavy curve without data is for water without additive. Since the Reynolds number is based on solvent (water) viscosity, the shift of the laminar data to the right is a direct measure of viscosity of the solution. Also, since the initial turbulent portion of the Polyox curve is shifted to the right by the same amount,

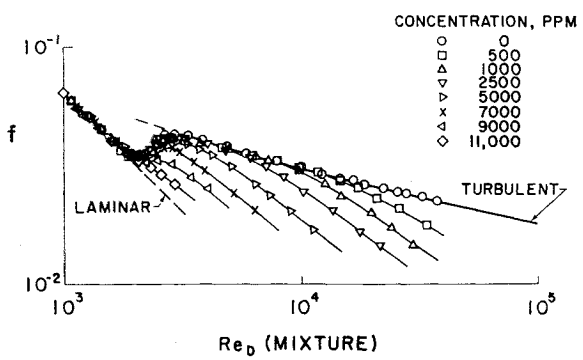

Fig. 4 Friction factor for aqueous solutions of Polyox-N750 in ½-in. pipe; Reynolds number based on mixture viscosity; temperature 71°F.

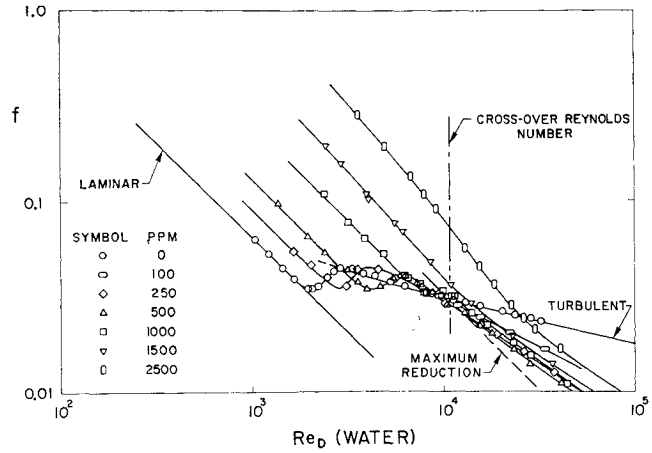

Fig. 5 Friction factor for aqueous solutions of Guar Gum in ½-in. pipe; Reynolds number based on water viscosity; room temperature.

non-Newtonian effects have not appeared in the viscosity even under the high shear rates in the viscous sublayer of the turbulent flow. The immediate important observation from the figure is that indeed the turbulent friction of the solution falls below that for the solvent, and in a rather rapid fashion. One may note also, however, that another minor drag-reduction region exists to the left of the diagram, but there owing to the increase in viscosity which requires proportionate increase in velocity for the same Reynolds number of transition. Drag increases are evident in the figure; not only in the laminar region owing to increase in viscosity, but also in the turbulent region owing to increase in viscosity. Thus, the drag reduction because of macromolecules occurs at sufficiently high Reynolds numbers when the flow is turbulent and continues to increase with increasing Reynolds number. Finally, observe in Fig. 2 that at 1500 ppm, transition of the laminar flow in the pipe is not delayed, while only the turbulence, after it is developed, is attacked. It should be mentioned here that plotting the data in terms of solvent viscosity permits immediate recognition of drag reduction; otherwise it would be necessary to compute it from viscosity measurement.

When higher concentrations are plotted on Fig. 2, the result is Fig. 3. Although the figure appears very busy, the intent is to prove that while the transition upswing continues to shift to the right, the drag reduction region pivots about a minimum cross-over point and is ultimately overtaken or

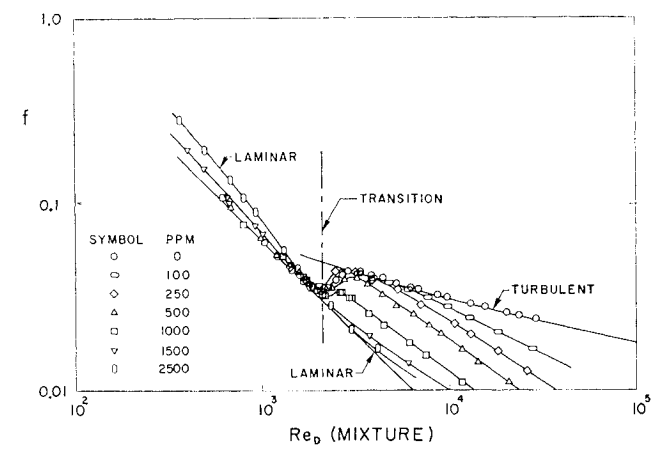

Fig. 6 Friction factor for aqueous solutions of Guar Gum in ½-in. pipe; Reynolds number based on mixture viscosity; room temperature.

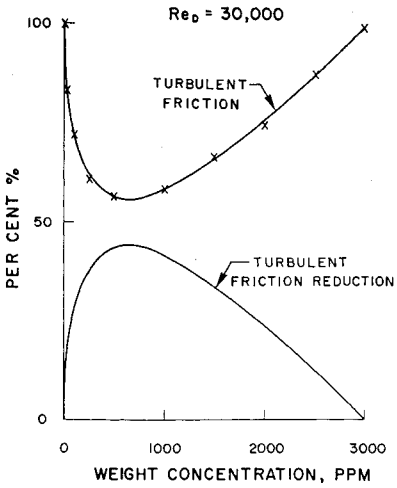

Fig. 7 Friction reduction for aqueous solutions of Guar Gum in ½-in. pipe; Reynolds number based on water viscosity; room temperature.

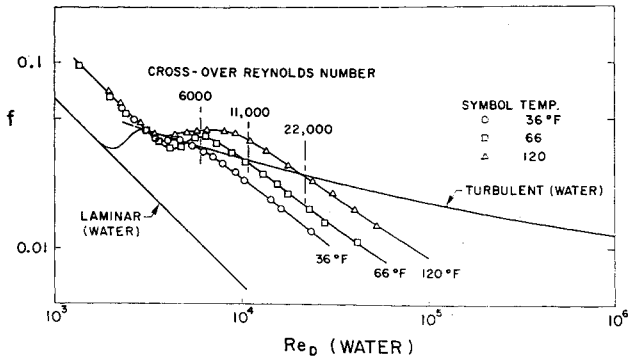

Fig. 9 Friction factor for 500 ppm aqueous solution of Guar Gum as a function of temperature; Reynolds number based on water viscosity; pipe diameter = 0.500 in.

washed out owing to increasing laminar friction. Newtonian viscous flow is obvious from the horizontal transition shift and parallel lines in the laminar region.

It is now instructive to plot the Reynolds number in terms of solution viscosity. This is done by merely shifting all curves back to the solvent laminar line, hence Fig. 4. Most remarkable is that the transition Reynolds number remains fixed, until eventually, at sufficiently high Reynolds number, the pipe is choked and the flow is held more and more laminar (although its drag could be greater than turbulent drag!). Another advantage of this type of plot is that it shows immediately the effect of the additive on the turbulent flow, for if there were no effect, all the data would fall on the single water curve. (In Fig. 3, the data for each additive concentration would have fallen on a line parallel to the water curve). It is recalled that this plot, however, does not indicate drag reduction as in Fig. 3, accordingly it does not display the cross-over point. But the threshold point of initial deviation from the solution curve is directly measurable.

Results of similar experiments using Guar Gum (molecular weight 220,000) are indicated in Figs. 5 and 6. How the friction reduction varies with concentration is seen in Fig. 7 at the arbitrary Reynolds number of 30,000. The sudden reduction and subsequent recovery owing to transition wash out are apparent. Further documentation on how additives damp the flow turbulence is exhibited in the dye pictures of Fig. 8.

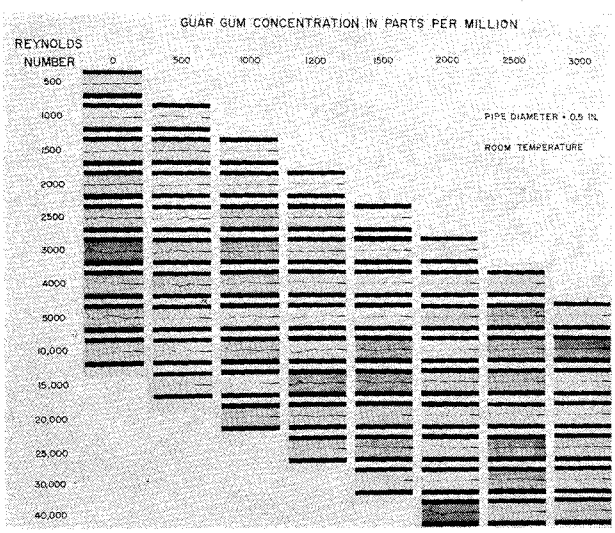

Fig. 8 Flow visualization of state of flow of aqueous solutions of Guar Gum in ½-in. pipe; Reynolds number based water viscosity; flow is from right to left.

Temperature Effect

Because it was desired to show that the turbulent drag reduction phenomenon was a function of the viscosity of the solvent for a given polymer, sets of experiments with Guar Gum were also carried out at temperatures 36°F and 120°F, in addition to the 66°F of Fig. 5. The friction factor data for 500 ppm are plotted in Fig. 9 where it is seen that the drag reduction phenomenon does indeed depend strongly on the solvent temperature as indicated by the different cross-over Reynolds numbers corresponding to each temperature. Thus, the friction-reducing effectiveness is greatly enhanced by reduction in temperature.

Fundamental to an understanding of the molecular interaction is the study of the variation of viscosity of the solution with concentration and temperature. Since the parallel laminar lines of Fig. 5 yield relative viscosities directly, the variation of viscosity μ with concentration p may be plotted as in Fig. 10. (The curvature in the laminar lines at the higher concentrations indicates the increasing presence of non-Newtonianism). The data of Fig. 5 being at 66°F yield the middle curve of Fig. 8. Now, further, since the spacing of the lines in Fig. 5 is proportional to the concentration, an exponential variation is suggested, whence,

$$\mu = \mu_0 \exp(1.3p/1000) \qquad (1)$$

wherein the constant was derived from the data. In this equation μ_0 is viscosity at zero concentration and p is concen-

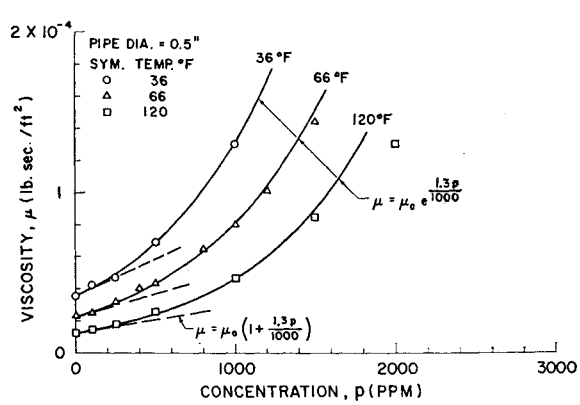

Fig. 10 Viscosity of aqueous solutions of Guar Gum as a function of temperature and concentration.

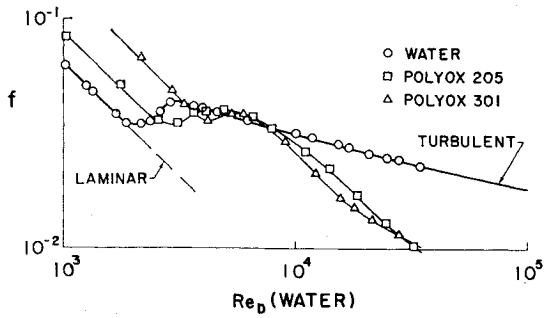

Fig. 11 Friction factor for 500-ppm aqueous solutions of Polyox 205 and 301 in ½-in. pipe; temperature 70°F.

tration in weight ppm. For small p, Eq. 1 reduces to

$$\mu = \mu_0[1 + (1.3/1000)p] \tag{2}$$

which has the linear form derived by Einstein in 1905 for infinitesimal spheres.[3] The viscosity data for the other temperatures also appear to follow the same law given by Eq. 1.

Molecular Weight Effect

While the previously studied polymers were quite different in their molecular structure, another pair of polymers to be discussed are apparently structurally similar except for length of chain, namely molecular weight. In Fig. 11, data are plotted for 500-ppm aqueous solutions of Polyox 205 (molecular weight 600,000) and Polyox 301 (molecular weight 4,000,000) at the same temperature of 70°F. Note that the cross-over Reynolds number is essentially the same for both, whereas their viscosities are not. How the viscosities vary relative to each other should be indicative of the manner in which the long chains act as they rotate and consequently distort the established shear flow. Figure 12 presents the data over a range of concentrations for the two Polyox's of relative length 4,000,000/600,000 = 6.7. The viscosity ratios are plotted in Fig. 13.

It will be seen that the viscosity-ratio curves can be made to collapse when the concentrations are inversely as the $\frac{2}{3}$ power of the molecular weights. Thus, it appears that for molecular chains, Eq. (2) should be written

$$\mu = \mu_0[1 + A(\bar{l}/d)^{2/3}(cN_0/M)\bar{l}d^2] \tag{3}$$

Here, c is mass concentration per unit volume, M is molecular weight, N_0 Avogadro's number, $\bar{l}$ the molecule length, d the molecule diameter, and A a constant. For rigid spheres,

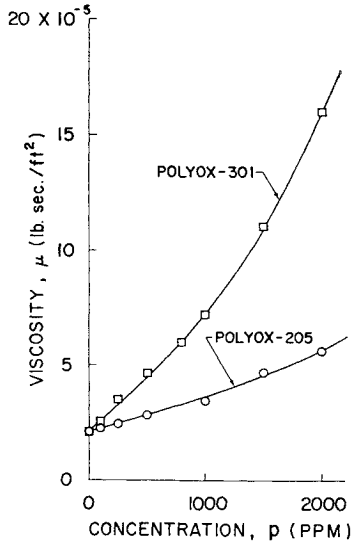

Fig. 12 Viscosity of aqueous solutions of Polyox 205 and 301; temperature 70°F.

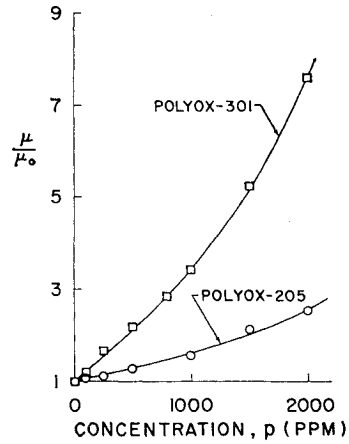

Fig. 13 Viscosity ratio of aqueous solutions of Polyox 205 and 301; temperature 70°F.

Einstein obtain theoretically

$$\mu = \mu_0[1 + (5\pi/12)(cN_0/M)d_s^3] \tag{4}$$

where d_s is sphere diameter. This equation is the same as

$$\mu = \mu_0[1 + \tfrac{5}{2}(\Delta v/v)] \tag{5}$$

with $\Delta v/v$ the total volume ratio of the spheres. It therefore appears that the factor $(\bar{l}/d)^{2/3}$ in Eq. (3) accounts for the manner in which the long flexible molecular chains sweep out paths in the flow. Again, from Eq. (3), since M is proportional to $\bar{l}$, for the same viscosity,

$$C_1 = C_2(M_2/M_1)^{2/3} \tag{6}$$

Pipe-Diameter Effect

In Fig. 14 are plotted friction factor data for 250-ppm aqueous solution of Guar Gum flowing in three sizes of pipe. A pipe-diameter effect is obvious, but this means that some other length is present which controls the turbulent drag reduction phenomenon. Such a fixed length can only be relative to the flow, hence the assumption of a fixed layer of thickness L in which eddying motion is damped by the entangled long molecules[4]; however, a laminar sublayer δ still exists which may be larger or smaller than the macrolayer L. If the Reynolds number is small enough such that $\delta > L$, then the sublayer stability will predominate. If the Reynolds number is large enough such that $\delta < L$, then the eddies in the remaining region between δ and L will be damped to a degree depending on the concentration of the polymer solution. Accordingly, the criterion for drag reduction onset (threshold) will be

$$\rho(\tau_w/\rho)^{1/2}L/\mu = \rho(\tau_w/\rho)^{1/2}D/\mu(L/D) = 11.6 \tag{7}$$

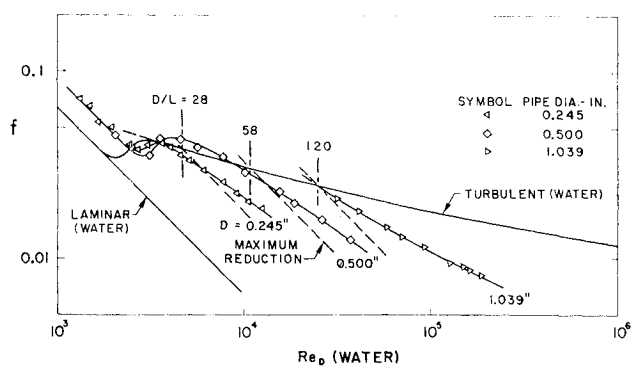

Fig. 14 Friction factor for 250-ppm aqueous solution of Guar Gum as a function of pipe diameter; Reynolds number based on water viscosity; room temperature.

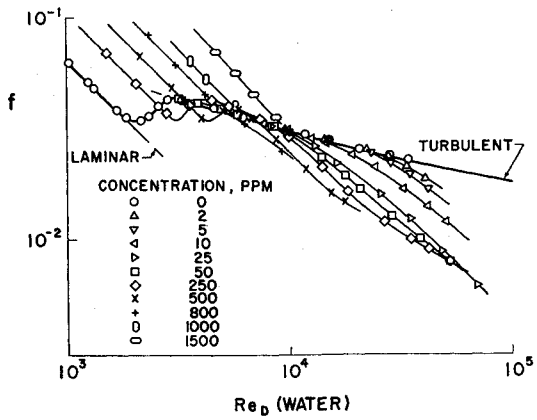

Fig. 15 Friction factor for aqueous solutions of Polyox 301 in ½-in. pipe; Reynolds number based on water viscosity; temperature 70°F.

from which, since friction factor $f = 8\tau_w/\rho V^2$ and $Re_D = \rho VD/\mu$,

$$Re_D f^{1/2} = 32.8\, D/L \tag{8}$$

In these equations, τ_w is wall shear stress, ρ fluid density, μ fluid viscosity, and V average velocity across the pipe. Now, for smooth pipes, the friction law is

$$1/f^{1/2} = -0.8 + 2\log_{10}[Re_D f^{1/2}] \tag{9}$$

Hence, with Eq. 8,

$$Re_D = 65.6(D/L)[1.1 + \log_{10}(D/L)] \tag{10}$$

the threshold Reynolds number at which damping of turbulent fluctuations begins with consequent drag reduction. Using Eq. (10) and the experimental cross-over Reynolds numbers of Fig. 14, the minimum value of L is found to be 0.22 mm for Guar Gum at room temperature. Thus, the resulting values of D/L are 28, 58, and 120 for the three pipes of Fig. 14.

Attention is called to the fact that L depends on both concentration and temperature, rather is a strong function of the mixture viscosity. Therefore, the threshold Reynolds number is a function of concentration and temperature, whereas the cross-over Reynolds number (minimum L) is apparently dependent only on temperature (Fig. 9). Hence, for drag reduction calculations, the minimum value of L (near-zero concentration) is usually sufficient. However, in some cases, this minimum L is not so well defined (see Fig. 15 of Figs. 15 and 16 for Polyox-301).

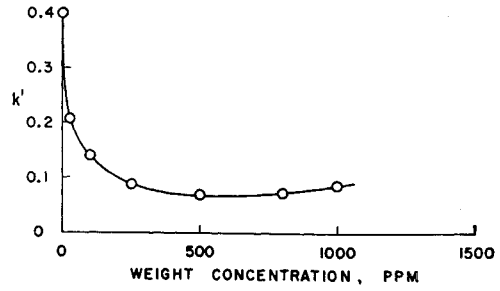

Fig. 17 Modified Kármán constant for aqueous solutions Guar Gum in ½-in. pipe; Reynolds number based on water viscosity; room temperature.

Velocity Profile

If it is assumed that the velocity profile in the intermediate turbulence damping zone between the distances L and δ can still be represented by a semilog law, then it is only necessary to modify the Kármán mixing-length constant in that region.[4] Thus, if the modified length is now written as $l = k'y$, where y is distance from the wall, the intermediate velocity profile is

$$u/(\tau_w/\rho)^{1/2} = 11.6 + (1/k')\ln[\rho(\tau_w/\rho)^{1/2}y/11.6\,\mu] \tag{11}$$

The constant represents the outer edge of the laminar sublayer where $u/(\tau_w/\rho)^{1/2} = \rho(\tau_w/\rho)^{1/2}\delta/\mu = 11.6$. But since the outer edge of the macromolecular zone is at $\rho(\tau_w/\rho)^{1/2}L/\mu$, the profile for the outer undamped fully turbulent region is then

$$u/(\tau_w/\rho)^{1/2} = 11.6 + (1/k')\ln[\rho(\tau_w/\rho)^{1/2}L/11.6\,\mu] + (1/k)\ln(y/L) \tag{12}$$

Thus, the entire profile is approximated by three intersecting curves.

Friction Factor

It is next easy to derive a friction factor formula for flow in a tube in terms of mean velocity V. Upon integration of Eq. (12) across the pipe, there results $u_m/V = 1 + 3.75\,(f/8)^{1/2}$ where u_m is the maximum velocity at $y = D/2$. Hence,

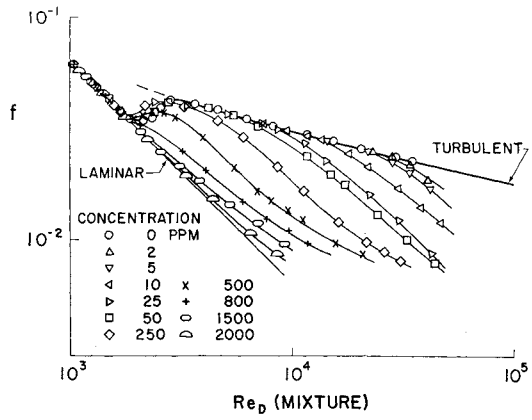

Fig. 16 Friction factor for aqueous solutions of Polyox 301 in ½-in. pipe; Reynolds number based on mixture viscosity; temperature 70°F.

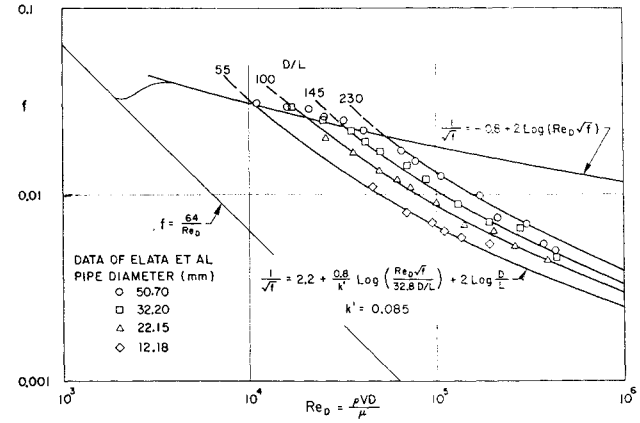

Fig. 18 Suppression of turbulence by additives; theory and experiment for 800-ppm aqueous solution of Guar Gum in various sized pipes.

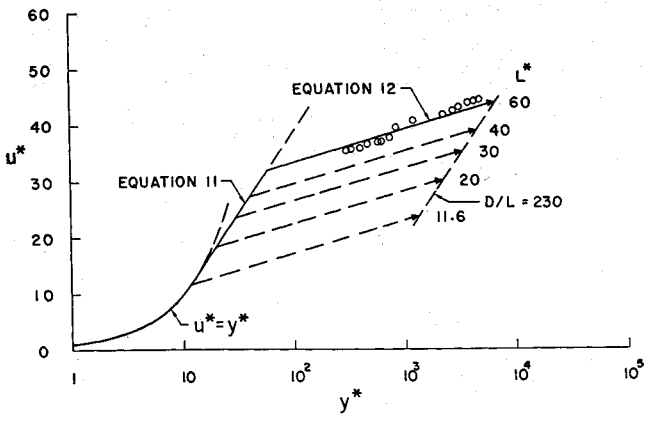

Fig. 19 Velocity profile for 800-ppm aqueous solution of Guar Gum in a 2-in. pipe.

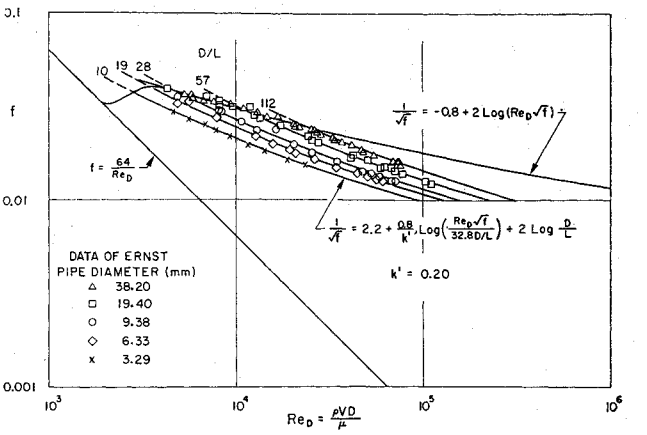

Fig. 20 Theory and experiment for 500-ppm aqueous solution of CMC—7H in various sized pipes.

with $k = 0.4$,

$$1/f^{1/2} = 2.2 + (0.8/k') \log_{10}[Re_D f^{1/2}/32.8\ D/L] + 2 \log_{10}(D/L) \quad (13)$$

in which the numerals have been rounded off to fit the Nikuradse pipe-friction data for pure water. When $k' = k = 0.4$, Eq. (13) reduces to Eq. (9) as expected.

A typical variation of k' with concentration can be readily obtained, say for Guar Gum of Fig. 5. This is done from Eq. (13), matching the data for each concentration of polymer, and having L (in this case 0.22 mm) from the cross-over point. Figure 17 shows such variation. The rapid fall in k' is immediately apparent, following somewhat a parabolic deficiency form at the smaller polymer concentrations. Note that the minimum value of k' is about 0.07 for this type of polymer. The reversal is because of the increase in viscosity with concentration, causing the laminar sublayer to fill up the pipe and stabilize the flow. On the other hand, the minimum k' such that Eq. (11) is tangent to the laminar sublayer is $k' = 1/\rho(\tau_w/\rho)^{1/2}\ y/\mu = 1/11.6 = 0.086$. Even lower values approaching zero should be attainable as the polymer concentration is greatly increased or longer molecules are used.

An explanation of the parabolic drag defect law is proposed as follows. Since the macromolecules are so long that they would overlap when they are distributed uniformly throughout the solvent, which occurs when $(cN_0/M)^{1/3}\bar{l} > 1$, it is assumed at the outset that the molecules align themselves end to end and therefore wind back and forth, etc., until the total length of molecules per unit volume is accounted for. Therefore it follows that the total length of molecules per unit volume is $cN_0\bar{l}/M$ of which $\frac{1}{3}$ are in one direction. The number of rods along each edge of the unit cube is then proportional to $(cN_0\bar{l}/M)^{1/2}$, and hence the spacing is proportional to $1/(cN_0\bar{l}/M)^{1/2}$. Any fluctuating turbulent velocities will then encounter $(cN_0\bar{l}/M)^{1/2}$ rods per unit distance which in turn will damp proportionately that much velocity. Therefore the remaining fluctuations will be proportional to $1 - Bc^{1/2}$, where B is a constant, and c is concentration of additive.

Experimental Verification of Theory

Data of Elata, Lehner, and Kahanovitz[5] for 800-ppm Guar Gum in various sized pipes are plotted in Fig. 18. It is seen that Eq. (13) has the proper form and fits the data very well when $L = 0.22$ mm and $k' = 0.085$. Particularly interesting is the observation that the completely independent data of Ref. 5 and of the present report for Guar Gum (Fig. 14) yield the same numerical value for L. Apparently the k's also agree.

Velocity profile data of Ref. 5 are shown in Fig. 19, and it appears that the fully turbulent portion of Eq. (12) passes through the data sufficiently well for the Reynolds number tested. In the figure the symbols are $u^* = u/(\tau_w/\rho)^{1/2}$, $y^* = \rho(\tau_w/\rho)^{1/2}y/\mu$, and $L^* = \rho(\tau_w/\rho)^{1/2}L/\mu$.

Data of Ernst[6] for 500-ppm Carboxymethylcellulose (CMC) (molecular weight 200,000) plotted in Fig. 20 appear to give further justification for the macromolecular damping layer concept developed in the present paper. Equation (13) fits quite well for $L = 0.34$ mm and $k' = 0.20$.

Asbestos Fibrils

Although the present paper concerns aqueous solutions of high polymers in the main, it should be of interest to display the results of friction factor measurement using very slender asbestos fibrils of length to diameter ratio 200:1. The diameter of the fibril is 0.125 μ or 250 Å so that the length is on the average about 50,000 Å. Figure 21 shows the data for various concentrations for flow in a $\frac{1}{2}$-in. tube. It is immediately obvious from the figure that the admixture of the fibrils increases the viscosity greatly in the laminar region (in fact the fabrils induce thixotropy) whereas no observable effect is produced on friction, increase or decrease, in the turbulent region of the flow. Thus, although transition slips somewhat probably owing to non-Newtonianism, the turbulent fluctuations are apparently unaffected. Apparently, this is a case where the fibrils do not interact with each other in the high-shear flow in the sublayer, so that

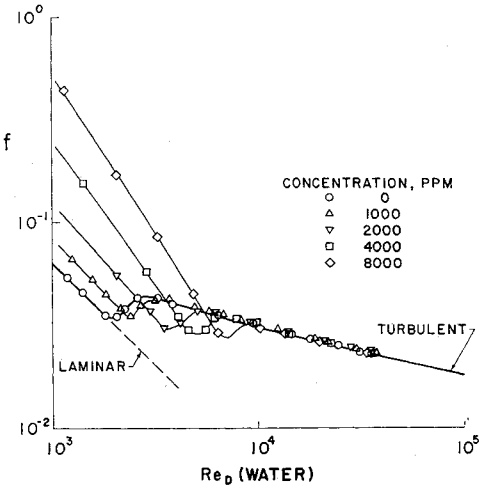

Fig. 21 Friction factor for aqueous mixture of calidria asbestos RG—144 in $\frac{1}{2}$-in. pipe; Reynolds number based on water viscosity; temperature 70°F.

there is practically no effect on solvent viscosity or turbulent fluctuations.

Conclusion

The main conclusion to be drawn from the previous discussion is that the effect of the polymers in solution is to damp the oscillations or eddies of turbulent flow, and that the size of eddy damped increases with the concentration. This apparently accounts for the choking out of turbulence in tubes at sufficiently high additive concentration. Thus, the additive has the property of a low-pass filter. The concept of a macromolecular fixed thickness per concentration within which velocity oscillations are damped is analogous to the hydraulic roughness of rough surfaces.

References

[1] Hoyt, J. W. and Fabula, A. G., "The Effect of Additives on Fluid Friction," NAVWEPS Rept. 8636, Dec. 1964, U.S. Naval Ordnance Test Station, China Lake, Calif.

[2] Wells, C. S., *Viscous Drag Reduction*, Plenum Press, New York, 1969.

[3] Einstein, A., *Investigations on the Theory of the Brownian Movement*, E. P. Dutton, New York.

[4] Van Driest, E. R., "The Damping of Turbulent Flow by Long-Chain Molecules," Scientific Rept. 67-2369, Sept. 1967, Air Force Office of Scientific Research.

[5] Elata, C., Lehner, J., and Kahanovitz, A., "Turbulent Shear Flow of Polymer Solutions," *Israel Journal of Technology*, Vol. 4, No. 1, 1966, pp. 87–95.

[6] Ernst, W. D, "Turbulent Flow of an Elasticoviscous Non-Newtonian Fluid," *AIAA Journal*, Vol. 5, No. 5, May 1967, pp. 906–909.

Engineering Notes

ENGINEERING NOTES are short manuscripts describing new developments or important results of a preliminary nature. These Notes cannot exceed 6 manuscript pages and 3 figures; a page of text may be substituted for a figure and vice versa. After informal review by the editors, they may be published within a few months of the date of receipt. Style requirements are the same as for regular contributions (see inside back cover).

Technological Interrelationships between Aerospace and Hydrospace

Otto Klima*
General Electric Company, Philadelphia, Pa.

Introduction

CURRENT technological pursuits in aerospace and hydrospace, although conducted in two distinct natural environments, reveal interrelationships with a certain commonality as well as a number of dissimilarities. These interrelationships can provide the engineer and scientist with a test and analytic expediency and sources of valid analogy applicable to either field. In general, both fields require equal technological skill. Unquestionably, there are sufficient similarities between the two fields that acquired knowledge may be utilized to the mutual benefit of personnel working in either aerospace or hydrospace. However, engineers and scientists schooled in one field are cautioned not to rush to the other with visions of providing a panacea for problems encountered by their counterparts there. To support these premises, this Note presents examples drawn from materials behavior, fluid mechanics and heat transfer, and solid body dynamics, all measured within the system context of weight constraint, time constraints, environmental phasing, life, reliability, and human safety. Finally, there is a brief commentary on the chronological development of each field.

Three years ago, Congressman Joseph E. Karth of Minnesota, offered this advice to the aerospace community: "While there are many specific technological areas in which space offers much promise in our assault on the oceans, I believe a note of caution is necessary. Study the field carefully and be patient . . . ."

Although, as the title of this Note suggests, there are possibilities and benefits of a transfer of knowledge from one field to the other, the aerospace field must approach hydrospace cautiously and, above all, with humility.

In viewing these technological interrelationships from a perspective which includes participation in both aerospace and ocean programs, it is difficult to see any broad array of ready-made spinoffs from one field to the other. A transfer of knowledge is possible. Some practical applications have occurred, especially from aerospace to hydrospace. Yet it seems that the most important transfers, and therefore the strongest area for interrelationships, have occurred in two areas, neither of which is purely technological. The cautionary note, therefore, should be: aerospace engineers and scientists should not presume to have off-the-shelf answers for problems confronting their hydrospace counterparts; and hydrospace engineers and scientists must not come to believe that they do.

Certainly aerospace-developed techniques and technologies have paved the way for better understanding and exploitation of the ocean environment. However, lessons learned from aerospace, rather than providing "pat" answers for hydrospace problems, offer the building blocks from which progress can be constructed in the hydrospace field. Therefore, in a very real way, aerospace research and development does offer hydrospace engineers and scientists a "way to go."

Technical Talent Pool

Consider, for instance, that the aerospace program in the United States created a technical talent pool unprecedented in the history of this or any other nation. There is now more technical competence available to attack a broader range of problems than at any time in history. This pool, of course, was not always available.

Presented as Paper 69-1089 at the AIAA 6th Annual Meeting and Technical Display, Anaheim, Calif., October 20–24, 1969; submitted December 12, 1969.

* General Manager, Re-entry and Environmental Systems Division. Associate Fellow AIAA.